

# MAGNETIC AND MAGNETOELASTIC UNIFORMITY MEASUREMENTS ON $\text{Fe}_{78}\text{Si}_7\text{B}_{15}$ AMORPHOUS RIBBONS

C. Petridis — A. Delatolas — E. Hristoforou

In this paper we present results on magnetic and magnetoelastic uniformity measurements on  $\text{Fe}_{78}\text{Si}_7\text{B}_{15}$  amorphous ribbons. The measurements are performed using an automatic instrumentation device, with the ability to determine the  $B(H)$  and  $\lambda(H)$  functions along the length of a ribbon with parametric control of field and frequency. The device has been calibrated with respect to standard Ni wires. According to these results, it has been determined that magnetic and magnetoelastic uniformity functions are in agreement and they are also subject to the history of the under test samples. These measurements may allow the structural non destructive evaluation on the under test samples in real time, which may be usable in industrial NDT testing and sensing applications.

Keywords: magnetoelasticity, magnetization, uniformity

## 1 INTRODUCTION

Amorphous materials produced by rapid quenching techniques are mainly used in the industry as cores for low-loss transformers, sensing elements for various kinds of sensors (measuring displacement, tension, magnetic field) and as shielding materials [1-3]. Most of these applications rely solely on the magnetic properties of the in use material, properties that are different along the length of the material because of the manufacturing process [4,5]. The need for magnetic uniformity testing is especially crucial in amorphous fibers and ribbons used in sensors, due to the fact that a change in the sensing element results in a change in the sensor response and may require a re-calibration of the sensor device [6].

Currently, amorphous ribbons are manufactured by melt-spun devices, amorphous wires by in-water rapid quenching and glass covered wires by crucible drawing. All of these manufacturing techniques are very sensitive to the slightest change in their operating parameters, affecting the end material. The dynamics of the manufacturing process are extremely difficult to model resulting in an uncertainty not only in the final material magnetic properties, but in the composition as well. Annealing processes are used to tailor the material to specific requirements in expense to extended final device manufacturing time.

Existing techniques for material evaluation include destructive metallographic measurements, ultrasonic testing and radiographic testing. These techniques determine the mechanical properties and evaluate the physical uniformity and possible flaws in the structure of the material. They are suitable only for out of production testing and with a limited amount of samples, due to the time they require and the cost involved, both in terms of money and man-hours. The magnetic properties evaluation is currently performed out of production also, because of the different magnetic requirements of the end-users of the materials. The manufacturer of a sensing device is responsible of measuring the coercive field and

saturation magnetization of an amorphous ribbon to see if it is acceptable for his application.

The motivation of this work is to study the feasibility and effectiveness of an in-line magnetic properties uniformity testing apparatus for the documentation of the magnetic properties of a magnetic fibre or ribbon during its manufacturing process. Due to the nature of the manufacturing process itself, such a testing apparatus is best located after the actual manufacturing procedure just before the winding of the final material. Thus it is possible to obtain a magnetic properties documentation sheet for the under test material in respect to its length and include it in the final product, be it ribbon, wire or glass covered wire.

The experimental setup used for the measurements is presented, along with a brief description of the measurement procedures. A more analytical description would be of no interest, since the methods used are well established and commonly used for the magnetic characterization of materials. Some indicative obtained results are presented next for the magnetization measurements, namely coercive field, remanence magnetization and saturation magnetization followed by the magneto-elastic measurement results. Because of the large amount of measured data a selective presentation is deemed necessary. The presented work concludes with a discussion on the obtained results.

## 2 EXPERIMENTAL SETUP

The device used for the uniformity measurements was designed so that the measurements of the  $B(H)$  and  $\lambda(H)$  functions could be performed on a continuous basis along the length of a long ribbon in order to inspect the spatial character of the magnetization and magnetostriction. The physical layout is much like that of a tape recorder with the amorphous ribbon as the metal tape and is presented in Fig. 1. A circular loop of ribbon was used because it was very easy to repeat the measurements for one sample with respect to a fixed 'start' along its length.

\* Laboratory of Physical Metallurgy, National Technical University of Athens, Zografou Campus, Athens 15780, Greece, eh@metal.ntua.gr

The  $B(H)$  loop is measured with the AC magnetometer technique and the  $\lambda(H)$  loop is extracted from the MDL response of the ribbon under test [7]. More specifically, for the  $B(H)$  loop an excitation coil of 220 turns was made, 13 cm long and 4 cm in diameter using 1 mm copper wire.

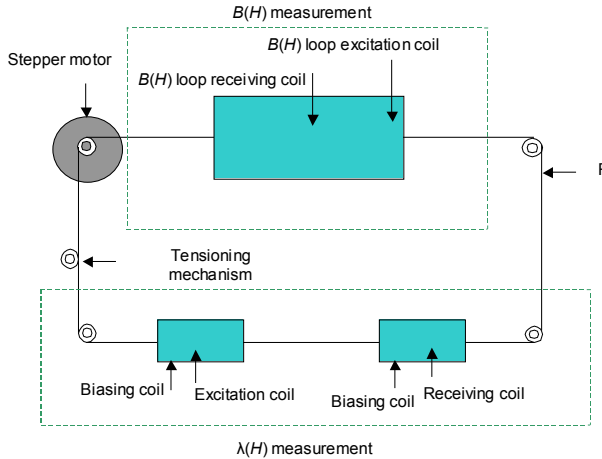


Fig. 1. Schematic layout of the measuring device.

Two additional coils (2 layers - 2 cm in length with the same wire) were wound on both ends of the excitation coil to improve the magnetic field homogeneity. The receiving coil depicted on figure 1 is actually two coils connected in series opposition, with the sample running directly the magnetization of the ribbon without the sinusoidal excitation superimposed. These two coils are identical in construction, 1 cm long with 20 layers of 0.1 mm copper wire and a rectangular area of 2 mm<sup>2</sup>. The signal from the receiving coils along with the excitation coil current is read with a digital oscilloscope and stored in a computer for further processing. This includes signal conditioning, noise removal and finally digital integration to obtain the  $B(H)$  loop.

The magneto elastic measurements were also performed along the length of the ribbon, using the MDL response technique [8,9]. Both the AC magnetometer technique for the  $B(H)$  loop and the MDL response technique for the  $\lambda(H)$  loop were chosen because they require no physical contact with the sample under measurement. For the  $\lambda(H)$  loop two sets of coils were constructed, a biasing - excitation coil assembly and a biasing - receiving coil assembly. Both biasing coils are 5 cm in length, 1 cm in diameter, single layer with 80 turns and are used for biasing the under measurement ribbon with a constant magnetic field locally producing a change in length  $\lambda_0$ . The excitation coil is 3 mm in length with 30 turns of 0.1 mm copper wire. The receiving coil is 2 mm in length with 300 turns of 0.01 mm copper wire. By applying a pulsed voltage to the excitation coil, a change in length  $\Delta\lambda$  is produced causing a magneto elastic wave to propagate along the ribbon and a voltage change in the receiving coil. If the pulsed voltage is kept constant in

frequency and amplitude, it is possible to measure  $\lambda_0$  by varying the amplitude of the biasing field. The signal from the receiving coil and the current from the biasing coils are measured and stored in a computer for further processing. The variable we are interested in is the change in the peak to peak voltage of the receiving coil with respect to biasing current, which, after digital integration is proportional to the  $\lambda(H)$  function.

The material actually used for the measurements was an amorphous melt spun Fe<sub>78</sub>Si<sub>7</sub>B<sub>15</sub> ribbon, 1mm wide and 25 $\mu$ m thick, mainly because of its ease of manufacturing, wide spread and fair magnetic properties. The ribbon was measured mostly in the as-cast form, but measurements after thermal treatment have been performed also.

### 3 EXPERIMENTAL RESULTS

#### Magnetization measurements

The magnetization measurements were performed along the length of the ribbon and gave wide variations in the coercive field and the other characteristics of the B-H loop. The  $B(H)$  loops for two random points, position '1' and '27', are illustrated in Figures 2 and 3 respectively, corresponding to the end and middle areas of the under test ribbons. In positions '1' and '27', the observed coercive fields were of 100 A/m and 50 A/m respectively (the x-axis dislocation is due to the non-compensation for the ambient magnetic field). These variations are attributed to a partial crystallization of the ribbon, and are highest at both ends of the ribbon. The reason for this is the increased amount of stresses at the ends of the ribbon, due to mechanical or electrical connection required by the experimental set-up. Figure 4 shows the dependence of the coercive field of the ribbon on the length of it, where such an end effect is more visible. By excluding the end effect a mean coercive field of 118 A/m was observed.

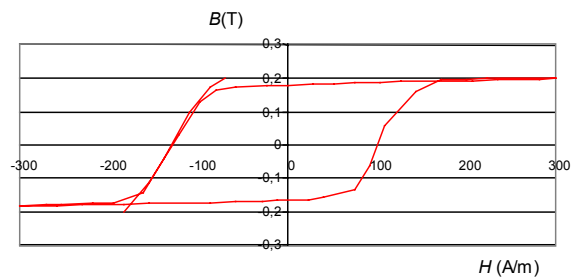


Fig. 2 The  $B(H)$  loop for the ribbon position marked as '1'.

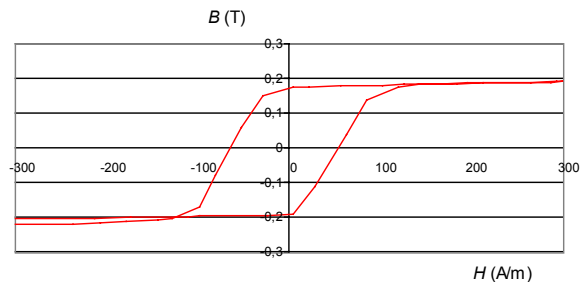


Fig. 3 The  $B(H)$  loop for the ribbon position marked as '27'.

On the other hand, the remanence magnetization and saturation magnetization show a remarkably better stability. Figure 5 shows the saturation magnetization with a mean value of 0.199 T and figure 6 shows the remanence magnetization with a mean value of 0.181 T.

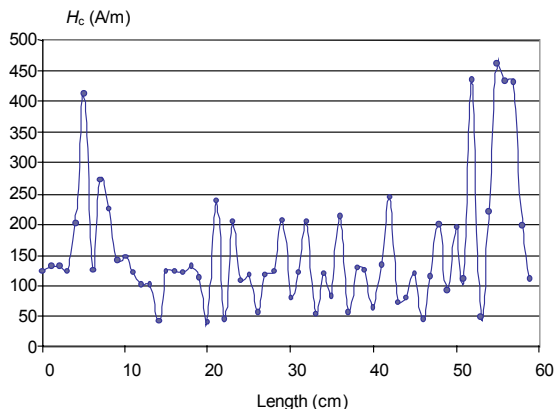


Fig. 4 Coercive field  $H_c$  versus ribbon length.

It should be noted that the actual values for saturation and remanence magnetization were not expected to be that close. The very small difference between them is due to the mechanical stressing of the ribbon from the experimental device: since the under test element is a positive magnetostrictive material, stress operates as an effective field, thus decreasing the coercive field and increasing the remanence value.

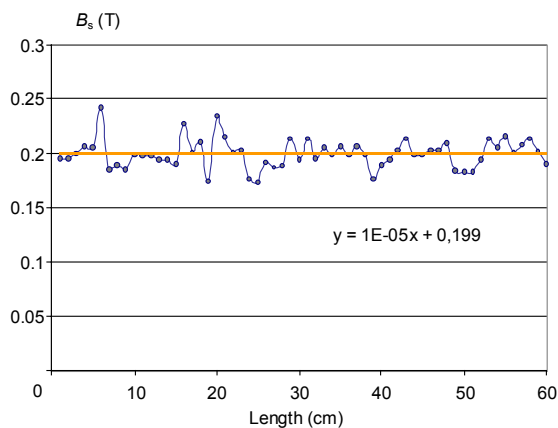


Fig. 5 Saturation magnetization versus ribbon length.

Magneto elastic measurements

Figure 7 shows the voltage output of the receiving coil - the integral of which is proportional to the  $\lambda(H)$  function - as a function of the applied magnetic field for four different ribbon samples (same composition, different batches). The same measurement for a single sample but for various points along its length is given in figure 8. These two figures reveal that the magneto elastic effect is a point effect and that it is different for the same material along its length mainly because of the differences in the crystalline structure. The total magnetostriction measured from capacitance or laser interferometer techniques is the sum of all the infinitesimal magneto elastic effects.

Another worth mentioning result was the hysteretic effect that was observed on occasion when measuring the  $\lambda(H)$  function for some samples. Figure 9 - and its integral, figure 10 - show the output voltage versus magnetic field for the same sample and at the same position, but for ascending and descending magnetic field. The figure shows clearly a hysteretic behavior observed repeatedly on some of the samples, but not all.

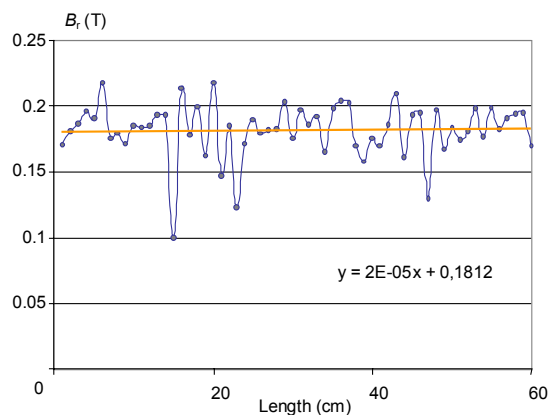


Fig. 6 Remanence magnetization versus ribbon length.

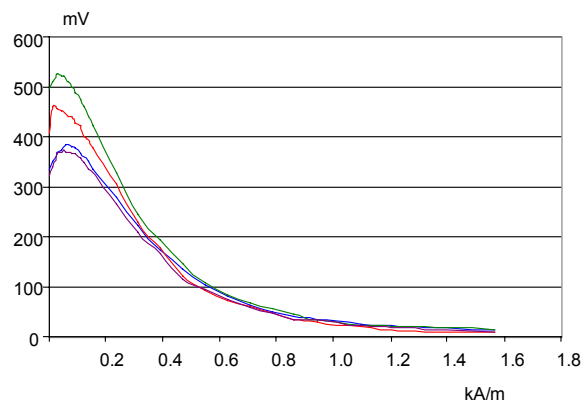


Fig. 7 Remanence magnetization versus ribbon length.

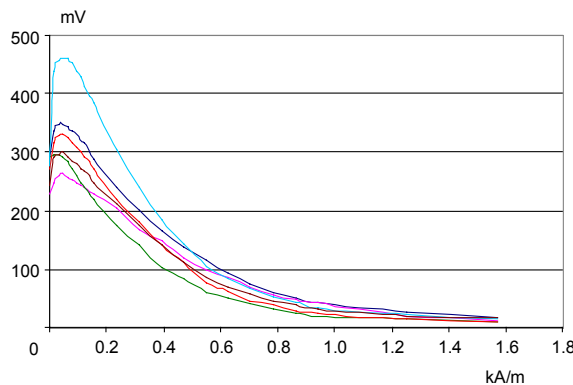


Fig. 8 Remanence magnetization versus ribbon length.

**4 DISCUSSION**

The large coercive field variations observed during the experiments is a result of the dependence of the coercive field to the crystalline structure of the material. A fully

crystalline material will have a large coercive field, as opposed to a completely amorphous one with the same composition.

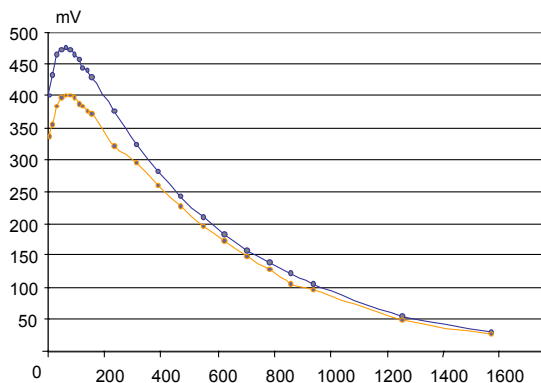


Fig. 9 Remanence magnetization versus ribbon length.

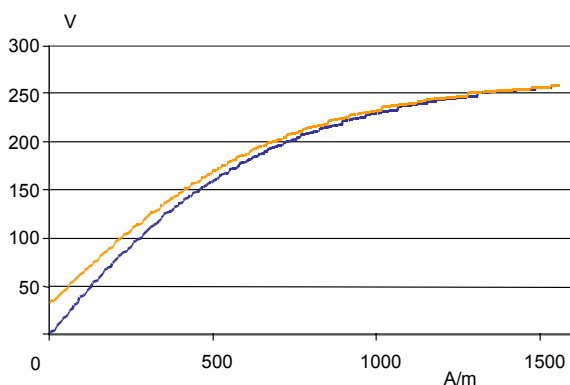


Fig. 10 Remanence magnetization versus ribbon length.

Various degrees of nano-crystallization fall in between in terms of coercive field value. The measurement of the coercive field with respect to length of the material is an indication of the crystalline structure of the material and can be used as a guide for further processing to obtain the required magnetic properties. Remanence magnetization and saturation magnetization are not affected so much from the crystalline structure, rather than the actual composition of the material. A stability in both remanence and saturation magnetization is expected from magnetic fibers or ribbons produced from the same mother alloy and is an indication of the composition for different runs comparisons. The crystalline structure is the main player in the  $\lambda(H)$  function of the material as well. It is responsible not only for the large variations in the  $\lambda(H)$  function along the length of a ribbon, but for the hysteretic effect observed in same samples. The presence of small nano-crystalline regions with different orientations can affect the response and induce a hysteretic effect. A TEM microscopic examination of the material along its length in comparison to the obtained  $\lambda(H)$  data

would be revealing of the actual correlation between crystalline structure and nano-crystalline region orientation to the magneto elastic response of magnetic ribbons.

As the description *amorphous metal* is subject to various estimations in respect to its meaning and the manufacturing techniques are not standardized for exact and repeatable results, a magnetic properties uniformity testing apparatus is deemed necessary, preferably at the manufacturing side, so that the end user can have accurate and detailed information for the material in question. The proposed device provides for a suitable means of magnetic and magneto elastic uniformity testing that can be installed both at the manufacturing side and the end-user side.

## REFERENCES

- Sensors<sup>+</sup>, IEEE Instr.&Meas. Mag. (June 2001) 28-32.
- [1] R. Hasegawa, Present status of amorphous soft magnetic alloys, Journal of Magnetism and Magnetic Materials, Volumes 215-216, 2 June 2000, pp 240-245
- [2] A.F. Cobeño, A.P. Zhukov, E. Pina, J. M. Blanco, J. Gonzalez, J. M. Barandiaran, Sensitive magnetoelastic properties of amorphous ribbon for magnetoelastic sensors, Journal of Magnetism and Magnetic Materials, Volumes 215-216, 2 June 2000, pp 743-745
- [3] F.B. Humphrey, Applications of amorphous wire, Materials Science & Engineering A: Structural Materials: Properties, Microstructure and Processing, Volume 179-80, Part 1, 1 May 1994, pp 66-71
- [4] M. Enokizono, I. Tanabe, T. Kubota, Localized distribution of two-dimensional magnetic properties and magnetic domain observation, Journal of Magnetism and Magnetic Materials, Volume 196, 1999, pp 338-340
- [5] C.K. Kim, Relationship between microstructure and magnetoelastic response in the magnetostrictive amorphous alloy Co<sub>47.4</sub>Fe<sub>31.6</sub>Si<sub>2</sub>B<sub>19</sub> after magnetic field annealing, Materials Science & Engineering B: Solid-State Materials for Advanced Technology, Volume B34, Issue 1, October 1995, pp 1-6
- [6] D. Bargiotas, V. Karagiannis, C. Manassis, Magnetoelastic uniformity of glass-covered wires used in magnetostrictive delay lines, Sensors and Actuators A: Physical, Volume 106, Issues 1-3, 15 September 2003, pp 80-83
- [7] Mogi Hisashi, Matsuo Yukio, Kumano Tomoji, AC magnetostriction hysteresis and magnetization direction in grain oriented silicon steel, IEEE Transactions on Magnetics, Volume 35, Issue 5 Part 2, September 1999, pp 3364-3366
- [8] E. Hristoforou, H. Chiriac and M. Neagu, An Alternative Method for Determining the  $\lambda(H)$  Function in Magnetostrictive Amorphous Alloys, Sensors and Actuators A, 67, p. 49-54, 1998
- [9] E. Hristoforou, H. Hauser, A. Ktena, Modeling of Magnetostriction in Amorphous Delay Lines, accepted, Journal of Applied Physics, 93, p. 8633-8635, 2003.

Received 28 June 2004